

Optimal Dynamic Buffer Management Using Optimal Control of Hybrid Systems

Wei Zhang and Jianghai Hu

School of Electrical and Computer Engineering
Purdue University, West Lafayette, IN 47907, USA.

{zhang70, jianghai}@purdue.edu

Abstract

This paper studies a dynamic buffer management problem with one buffer inserted between two interacting components. The component to be controlled is assumed to have multiple power modes corresponding to different data processing rates. The overall system is modeled as a hybrid system and the buffer management problem is formulated as an optimal control problem. Different from many previous studies, the objective function of the proposed problem depends on the switching cost and the size of the continuous state space, making its solutions much more challenging. By exploiting some particular features of the problem, the best mode sequence and the optimal switching instants are characterized analytically using some variational approach. Simulation result based on real data shows that the proposed method can significantly reduce the energy consumptions compared with another heuristic scheme in several typical situations.

I. INTRODUCTION

Dynamic buffer management (DBM) is an effective power management technique that can reduce the power consumptions of electronic devices by inserting buffers among interacting components. The buffer insertion makes it possible to turn off underutilized component at appropriate times without affecting the service for the other components, thus reducing the system power consumption. The optimal buffer size resulting in the largest power reduction is derived in [1], [2], [3] for some simple DBM problems. A major limitation of these studies is that they all assume that the components to be controlled have only two power modes, “on” and “off”. However, in practice, many components can work in more than two power modes, such as the variable speed processors ([4]) and the multi-speed disks ([5]). For such a component, instead of completely turning it off, one can properly design a switching strategy, namely the scheduling of different power modes of the component, to further reduce its power consumption.

This paper studies a more general DBM problem, where the component to be controlled has multiple power modes. Since different power modes correspond to different data accumulation/depletion rates in the buffer, the overall system is perfectly modeled as a piecewise-constant hybrid system, or more accurately, a multi-rate automata ([6]). The DBM problem is thus formulated as an optimal control problem of the underlying hybrid system.

Optimal control of hybrid systems is a challenging research topic that has attracted many researchers. In [7], a unified framework is formulated for optimal control of hybrid systems; some conceptual algorithms based on the Bellman equation are also proposed for computing the optimal control policies. A similar idea is employed in [8], where a more detailed algorithm based on the discretization of the continuous state space is developed to solve the Bellman inequality. In [9], [10], a two-stage optimization method is proposed for switched systems, where in the first stage the optimal continuous input is computed for a fixed switching strategy and then in the second stage the dynamic programming algorithm is used to compute the best switching strategy. In parallel with these dynamic-programming-based approaches, variational methods have also been extensively studied. In [11], [12], the maximum principle is generalized to solve a time optimal control and a linear quadratic control problem for switched systems with linear subsystems. Some more general versions of the maximum principle for hybrid systems are proved in [13] and [14]. Variational approaches are also used in [15], [16] to derive necessary conditions for the optimal switching instants and/or the optimal continuous control input for switched systems with a fixed switching sequence. Although an algorithm for updating the switching sequence is discussed in [16], finding the best switching sequence is still an NP-hard problem. More recently, [17] propose a way of embedding a switched system into a larger family of systems, whose solutions, obtained by the traditional optimal control methods, can be used to construct the optimal control of the switched systems without enumerating the switching sequences. Besides these theoretical works, applications of the optimal control theory of hybrid systems in various practical contexts have also been well studied. The problems in this category as in [18], [19], [20], [21], usually deal with particular model structures and cost functions that often enable one to find better analytical and numerical solutions. The optimal control problem considered in this paper falls into this category.

Despite the richness of the literature in this field, the problem studied in this paper can not be directly solved using the existing methods as it has the following distinct features: (i) transitions among discrete modes depend on the evolution of the continuous state; whereas many previous studies ignore such dependency; (ii) the switching (mode) sequence is a decision variable that cannot be assumed fixed; (iii) the switching cost ignored in most previous papers is an important part of our cost function; (iv) the

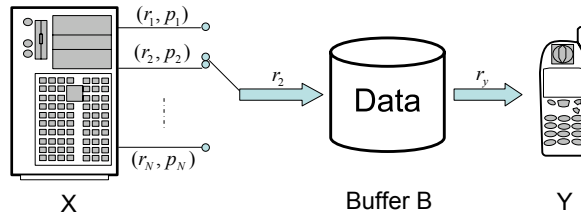


Fig. 1. System Configuration

buffer size that determines the range of the continuous states is variable, indicating that both the optimal control and the optimal size of the continuous state space are to be designed at the same time. Few existing results have addressed all of these issues.

The main contributions of this paper are the following: (i) Hybrid system framework is successfully applied to model the DBM problem, which is an important problem in the low power design of embedded systems. (ii) Two practically important DBM problems are formulated as optimal control problems of a piecewise-constant hybrid system and solved analytically through a variational approach. (iii) Several issues of implementing the proposed optimal strategy in practical systems are addressed. The results are also verified through some simulations based on real data.

The rest of this paper is organized as follows. In Section II, two DBM problems are introduced and formulated as optimal control problems of a piecewise constant hybrid system. In Section III, several operations on hybrid trajectories are introduced. These operations are then used in Sections IV and V to derive the optimal solutions. Two simulation examples are given in Section VI to illustrate the effectiveness of the optimal strategies. Concluding remarks and future research directions are discussed in Section VII.

II. PROBLEM FORMULATION

A. System Description

Consider two interacting components X and Y as shown in Fig. 1, where X produces data for Y to consume. Suppose that Y is always “on” and consumes data at a constant speed r_y . On the other hand, assume that X has N different operation modes where in mode i , $i = 1, 2, \dots, N$, it produces data at a constant speed r_i and consumes power p_i . Without loss of generality, assume $r_1 < r_2 < \dots < r_N$. Usually, a lower data rate corresponds to a lower power consumption; thus we require $p_1 < p_2 < \dots < p_N$. Denote by I and J the sets of indices whose corresponding data rates are greater and smaller than r_y , respectively,

i.e.,

$$I = \{i \mid r_i > r_y, i = 1, \dots, N\},$$

and $J = \{j \mid r_j < r_y, j = 1, \dots, N\}.$

Assume that both I and J are nonempty, i.e., $r_N > r_y > r_1$. Note that we ignore the degenerate case where r_y can be perfectly matched by one of the power modes of X , since in this case no buffer is needed and the DBM problem becomes trivial. A mode σ is called an *ascending mode* if $\sigma \in I$ and a *descending mode* otherwise. To ensure smooth operation, a buffer B with capacity Q is inserted between X and Y . See Fig. 1 for the configuration of the overall system.

Many real-world applications can be described by the above system. One simple example is the data-copying process, where a device Y copies data from a hard drive X . The hard drive has two power modes “on” and “off”. If the data rate of the hard drive is faster than that of Y , then X can be turned off during some time intervals to save energy. In this case, the system memory, which serves as the buffer B in our model, is needed to temporarily store the data from X for later delivery. As another example, consider the video playing process. Let X be the Intel Xscale processor ([22]) that can operate on multiple voltages corresponding to different speeds r_i 's and powers p_i 's; let Y be a video card that demands data from X at a constant speed, say 30frame/sec. To ensure smooth operation, the system memory is needed as a buffer to store the data that has been decoded by X but yet to be displayed by Y . Thus, the abstract system as shown in Fig. 1 represents a class of practical systems. Minimizing the power consumption of such a system has important practical implications.

B. Hybrid System Model

The above problem can be modeled as a hybrid system H . The discrete state space of H consists of N modes: $S = \{1, 2, \dots, N\}$, corresponding to the operation modes of X . The continuous state $q(t)$ is defined as the amount of data stored in the buffer B , and is thus required to take values in the interval $[0, Q]$. The evolution of $q(t)$ is determined by the speed difference between the two components, i.e., $\dot{q}(t) = r_i - r_y$ for mode i . As a physical constraint, there can be no buffer underflow or overflow. Thus, we require that whenever $q(t)$ hits the boundary of its domain, namely, $q(t) = 0$ or Q , the system must transit to another mode that can bring $q(t)$ back to the inside of $[0, Q]$. Except for this, there are no other transition rules and guard conditions. The reset map of the system is trivial, i.e., there is no jump in $q(t)$ at the transition instant.

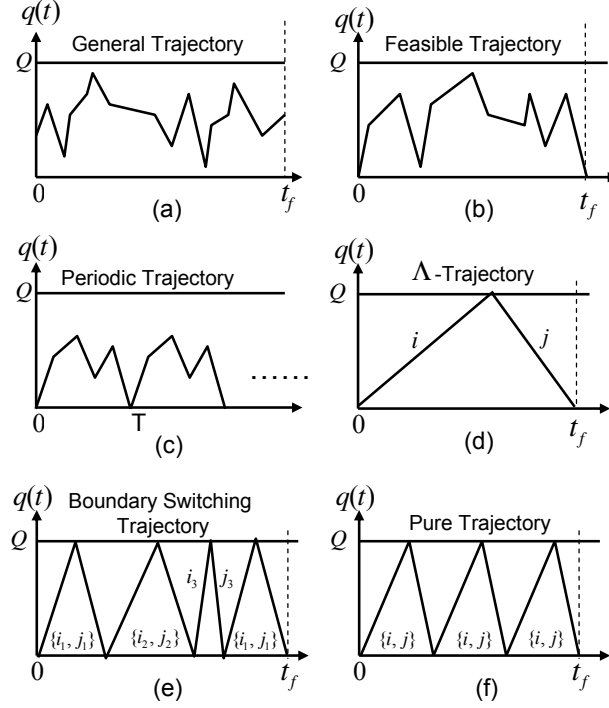


Fig. 2. Hybrid trajectories

Given a time period $[0, t_f]$, the behavior of the above system can be uniquely determined by the switching strategy $\sigma : [0, t_f] \rightarrow S$, which determines the active mode of the system over $[0, t_f]$. The overall trajectory $z(t) = (q(t), \sigma(t))$ of the hybrid system consists of the trajectories of the continuous state $q(t)$ and the discrete state $\sigma(t)$. For a given initial value $q(0)$, the system is governed by the following differential equation:

$$\frac{dq(t)}{dt} = r_{\sigma(t)} - r_y, \quad \forall t \in [0, t_f]. \quad (1)$$

In this paper, we study the power consumption of the whole process of transferring a certain amount of data from X to Y. It is thus required that the system must start with an empty buffer at $t = 0$ and end up with an empty buffer at $t = t_f$ when Y have received all the data produced by X. This yields two boundary conditions for the continuous state, namely, $q(0) = 0$ and $q(t_f) = 0$. The hybrid trajectories that satisfy these two conditions are called *feasible trajectories* (See Fig. 2-(b)).

Assume that there is a partition of $[0, t_f]$, $t_0 = 0 \leq t_1 \leq \dots \leq t_n = t_f$, for some $n \geq 0$, so that $\sigma(t) \equiv \sigma_i \in S$ is constant in each subinterval $[t_{i-1}, t_i]$, $i = 1, \dots, n$. The sequence $(\sigma_1, \dots, \sigma_n)$ is called

the *switching sequence* and (t_0, \dots, t_{n-1}) is called the *switching instants*¹.

A hybrid trajectory $z(t) = (q(t), \sigma(t))$ over $[0, \infty)$ is called *periodic* with period T if $q(t+T) = q(t)$ and $\sigma(t+T) = \sigma(t)$ for all $t \in [0, \infty)$. For such a trajectory, denote by n_T the number of switchings in each period. For example, $n_T = 5$ for the trajectory in Fig 2-(c).

A feasible trajectory is called a Λ -*trajectory* if it consists of one ascending mode i and one descending mode j with exactly two switchings as shown in Fig 2-(d). The pair of modes $\{i, j\}$ in a Λ -trajectory is called a Λ -*pair*.

A feasible trajectory $z(t) = (q(t), \sigma(t))$ with switching instants (t_0, \dots, t_{n-1}) is called a *boundary-switching trajectory (BST)* if $q(t_i) = Q$ or 0 for any $i = 0, \dots, n-1$. In other words, a BST only switches at the boundary of the range of $q(t)$. Denote by Ω the class of all BST's. Every BST can be decomposed into a series of Λ -trajectories with the same buffer size. Denote by n_p the number of *distinct* Λ -pairs in a BST. For example, $n_p = 3$ for the BST in Fig 2-(e). A BST is called *pure* if $n_p = 1$ and is called *mixed* otherwise. In other words, a pure trajectory must be a BST and is obtained by repeating a Λ -trajectory for a certain number of times (See Fig. 2-(f)).

The power consumption of a given hybrid trajectory $z(t) = (q(t), \sigma(t))$ consists of three parts: the *running power*, namely the power consumed by component X^2 , the *switching power* and the *buffer power*. Note that $p_{\sigma(t)}$ is the instantaneous power of X at time t . Thus the average running power over $[0, t_f]$ is $\frac{1}{t_f} \int_0^{t_f} p_{\sigma(t)} dt$. Assume that switchings among different modes consumes the same amount of energy k_s^3 . Then the average switching power over $[0, t_f]$ is nk_s/t_f , where n is the number of switchings in the trajectory z . The buffer power includes the static buffer power and the dynamic buffer power. The static buffer power is proportional to the buffer size while the dynamic buffer power only depends on the actual amount of data in the buffer. Since the dynamic buffer power is much smaller than the static one, in this paper, we only consider the static buffer power and denote it by $p_b Q$, where p_b is a positive constant and Q is the buffer size. Thus the total average power of the system during $[0, t_f]$ can be written as

$$\bar{P}(z; Q, t_f) = \frac{1}{t_f} \int_0^{t_f} p_{\sigma(t)} dt + \frac{nk_s}{t_f} + p_b Q, \quad (2)$$

¹The system is turned on at $t = 0$. Hence, we assume that there is always a switching at $t = 0$ and ignore the switching, if any, at $t = t_f$ for all trajectories.

²The power of Y is ignored in this paper since it is a constant independent of the switching strategy.

³There may exist other switching penalties, such as the switching delay penalty. To simplify discussion, we assume that all the switching penalties are transformed to an equivalent energy cost and incorporated into k_s .

and the total energy associated with $z(t)$ during $[0, t_f]$ is

$$E_\sigma(z; Q, t_f) = \int_0^{t_f} p_{\sigma(t)} dt + nk_s + p_b Q \cdot t_f.$$

The three terms on the right hand side of the above equation represent the *running energy*, the *switching energy*, and the *buffer energy*, respectively.

C. Problem Statements

The goal of this paper is to find a feasible trajectory that can finish a given task with the least energy consumption. For some applications, the amount of data to be transferred to Y is known *a priori*. In this case, t_f is a given constant which equals to the amount of data to be transferred divided by the data rate of Y. The energy minimization problem can be formulated as the following optimal control problem of the hybrid system H.

Problem 1: $\min_{z, Q} \bar{P}(z; Q, t_f)$ subject to the constraints: (i) $z(t) = (q(t), \sigma(t))$ satisfies equation (1); (ii) $q(t) \in [0, Q]$, $\forall t \in [0, t_f]$ and $q(0) = q(t_f) = 0$; (iii) $\sigma(t) \in S$, $\forall t \in [0, t_f]$.

Problem 1 requires the exact knowledge of t_f . However, in some applications, the time horizon t_f is not known *a priori*. For example, consider that a network card (component X) downloads a live video broadcast from the internet and at the same time sends the received data to a video card (component Y). The t_f in this example may not be known until X receives the last frame. In this case, we are usually interested in periodic strategies that are easy to implement and whose power can be computed even without the knowledge of t_f . Therefore, another meaningful problem is to find the optimal periodic trajectory with the least average power consumption.

Let $z(t)$ be a periodic trajectory with $(\sigma_1, \dots, \sigma_{n_T})$ and (t_0, \dots, t_{n_T-1}) as the switching sequence and switching instants during the first period $[0, T]$, respectively. Note that the periodic trajectory has an infinite length, i.e., $t_f = \infty$. The average power of z is the same as its average power during the first period, i.e.,

$$\bar{P}(z; Q, \infty) = \bar{P}(z; Q, T) = \frac{1}{T} \left(\sum_{i=1}^{n_T} p_{\sigma_i} \tau_i + n_T k_s \right) + p_b Q,$$

where $\tau_i = t_i - t_{i-1}$. Since every feasible solution must start with zero buffer, it follows that $q(T) = q(0) = 0$. Different from Problem 1, to find the best periodic solution, one not only needs to optimize the switching sequence and switching instants, but also needs to find the best period T . This is formulated as the following problem.

Problem 2: $\min_{z,Q,T} \bar{P}(z; Q, T)$ subject to the constraints: (i) $z(t) = (q(t), \sigma(t))$ is periodic with period T and satisfies equation (1); (ii) $q(t) \in [0, Q]$, $\forall t \in [0, T]$ and $q(0) = q(T) = 0$; (iii) $\sigma(t) \in S$, $\forall t \in [0, T]$.

Remark 1: The two problems in this section are independent of each other and serve different purposes. Problem 1 is suitable for the case where the value of t_f is known exactly before the system starts operating. On the other hand, for unknown t_f , Problem 2 prepares for the worst case by assuming $t_f = \infty$ and only focuses on infinite-length periodic strategies. However, for real applications the time horizon t_f must be finite. Thus, when the solution of Problem 2 is applied to a real system, only part of the strategy will be used. See Section IV-C for implementation details of periodic strategies.

For any optimal solutions to Problem 1 and 2, to avoid the unnecessary power consumption by the unused buffer space, Q should be chosen as small as possible so that the buffer is full at least once during $[0, t_f]$. In addition, since $q(t) \geq 0$ and $q(0) = 0$, the following lemma follows immediately.

Lemma 1: If $z(t) = (q(t), \sigma(t))$ is an optimal solution to Problem 1, then

$$\min_{t \in [0, t_f]} q(t) = 0, \quad \text{and} \quad \max_{t \in [0, t_f]} q(t) = Q.$$

This condition also holds for Problem 2 with t_f replaced by T .

According to Lemma 1, the optimal buffer size is completely determined by a given trajectory $z(t)$. From now on, we will call Q a *valid buffer size* of z if $\max q(t) \leq Q$ and the *optimal buffer size* of z if equality holds.

The rest of this paper is devoted to deriving analytical solutions to the two problems formulated in this section. Specifically, we will prove that: (i) the optimal solutions to both problems must be boundary-switching trajectories (BST's); (ii) the optimal pure periodic trajectory (OPPT) with $n_p = 1$ is an optimal solution to Problem 2 for an arbitrary n_p ; (iii) the optimal pure trajectory (OPT) with length t_f and $n_p = 1$ is an optimal solution to Problem 1 for an arbitrary n_p ; (iv) the OPT is different from the OPPT in general and will converge to the OPPT as t_f goes to infinity. Although we consider all feasible trajectories as candidate solutions, the above results enable us to only focus on pure (periodic) trajectories in finding the optimal solutions. Since a pure trajectory involves only one (distinct) Λ -pair and only switches when $q(t)$ is 0 or Q , the OPT and OPPT, which are optimal solutions to Problems 1 and 2, can be easily characterized analytically.

III. OPERATIONS ON HYBRID TRAJECTORIES

In this section, we introduce some important operations that can transform an existing trajectory to a new one while preserving certain properties. These operations play an important role in deriving the

optimal solutions to Problems 1 and 2.

A. Cropping

Cropping, denoted by $\mathcal{C}_{a,b}[\cdot]$, is an operation that obtains a new trajectory by trimming off the uninteresting parts of the original trajectory. For example, the cropped trajectory $\mathcal{C}_{a,b}[z]$ will only keep the part of $z(t)$ where $t \in [a, b]$, i.e.,

$$\mathcal{C}_{a,b}[z](t) = z(t + a), \quad \text{for } t \in [0, b - a].$$

B. Joining

Joining, denoted by $\mathcal{J}[\cdot, \dots, \cdot]$, is an operation that obtains a new trajectory by putting several finite-length trajectories together. For example, $\mathcal{J}[z^{(1)}, z^{(2)}]$ corresponds to a new trajectory obtained by appending $z^{(2)}$ to the end of $z^{(1)}$. More precisely,

$$\mathcal{J}[z^{(1)}, z^{(2)}](t) = \begin{cases} z^{(1)}(t) & , t \in [0, t_f^{(1)}] \\ z^{(2)}(t - t_f^{(1)}) & , t \in [t_f^{(1)}, t_f^{(1)} + t_f^{(2)}] \end{cases},$$

where $t_f^{(1)}$ and $t_f^{(2)}$ are the lengths of $z^{(1)}$ and $z^{(2)}$, respectively. To prevent introducing discontinuities, it is required that $z^{(1)}$ and $z^{(2)}$ have consistent boundary conditions, i.e., $q^{(1)}(t_f^{(1)}) = q^{(2)}(0)$, where $q^{(1)}$ and $q^{(2)}$ are the continuous states of $z^{(1)}$ and $z^{(2)}$, respectively. Denote by $\mathcal{J}_m[z]$ a special joining operation that repeats the trajectory z satisfying $z(0) = z(t_f)$ for m times, i.e.,

$$\mathcal{J}_m[z] = \mathcal{J}[\underbrace{z, \dots, z}_{m \text{ } z's}].$$

C. Periodic Extension

Periodic extension, denoted by $\mathcal{P}[\cdot]$, is an operation that obtains a periodic trajectory by repeating a given trajectory z for infinitely many times. Mathematically, $\mathcal{P}[\cdot]$ can be defined in terms of the joining operation as $\mathcal{P}[z] = \mathcal{J}_\infty[z]$. For a trajectory $z(t)$ of length t_f , $\mathcal{P}[z](t + l \cdot t_f) = z(t)$ for all $t \in [0, t_f]$ and any nonnegative integer l .

D. Scaling

For an arbitrary hybrid trajectory $z(t) = (q(t), \sigma(t))$, the scaling operation with parameter $c > 0$ is defined as

$$\mathcal{S}_c[z](t) = (cq(t/c), \sigma(t/c)).$$

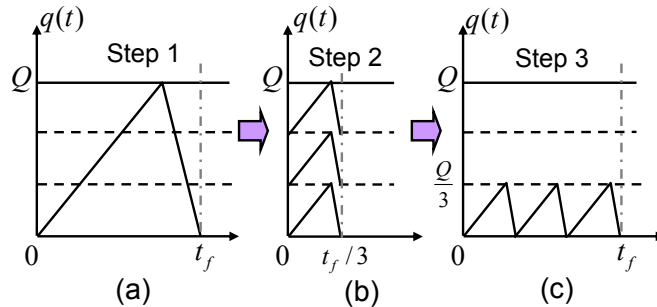


Fig. 3. Folding with $m = 3$

If $z(t) = (q(t), \sigma(t))$ is a hybrid trajectory in $[0, t_f]$ with buffer size Q , switching sequence $(\sigma_1, \dots, \sigma_n)$ and switching instants (t_0, \dots, t_{n-1}) , then $\mathcal{S}_c[z]$ is a hybrid trajectory in $[0, ct_f]$ with buffer size cQ , switching sequence $(\sigma_1, \dots, \sigma_n)$ and switching instants (ct_0, \dots, ct_{n-1}) . In other words, $\mathcal{S}_c[z]$ follows exactly the same switching sequence as z , but the time it spends in each mode before switching to a new one is scaled by a factor of c . An important property of the scaling operation is that it does not change the running power of a trajectory. It can be easily verified that the total average power of $\mathcal{S}_c[z]$ is

$$\bar{P}(\mathcal{S}_c[z]; cQ, ct_f) = \bar{P}(z; Q, t_f) + \frac{(1-c)nk_s}{ct_f} + p_b(c-1)Q. \quad (3)$$

E. Folding

Folding operation, denoted by $\mathcal{F}_m[\cdot]$, is only defined for the Λ -trajectories. It obtains a pure trajectory with $2m$ switchings from a Λ -trajectory with 2 switchings. Fig. 3 illustrates a 3-fold folding for a Λ -trajectory $z(t)$. The operation consists of the following three steps. First, the range of $z(t)$ is divided evenly into 3 sections. Each section corresponds to two segments of the trajectory; one is ascending and the other one is descending. Then by appending each descending segment to the end of the corresponding ascending one, a new Λ -trajectory is obtained in each section. Finally, all the three Λ -trajectories are joined together to obtain the final trajectory as shown in Fig. 3-(c).

If Q is the optimal buffer size of $z(t)$, then $\mathcal{F}_m[z]$ contains $2m$ switchings and has an optimal buffer size Q/m . In fact, any finite-length pure trajectory (e.g. Fig 3-(c)) can be thought of as obtained from a Λ -trajectory (e.g. Fig 3-(a)) through the folding operation with certain parameter m .

F. Switching Instant Perturbation (SIP)

Switching instant perturbation is defined only for two-switching trajectories, namely the trajectories (may not be feasible in general) with exactly two switchings. Let $z(t) = (q(t), \sigma(t))$ be a two-switching

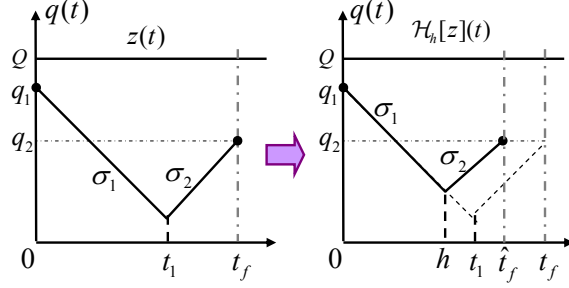


Fig. 4. Switching instant perturbation $\mathcal{H}_h[z]$ with $h < t_1$

trajectory with switching sequence (σ_1, σ_2) , switching instants $(0, t_1)$ and buffer size Q . Suppose that $q(0) = q_1$, $q(t_f) = q_2$. Denote by $\mathcal{H}_h[z] = (\hat{q}(t), \hat{\sigma}(t))$ the SIP of z . Roughly speaking, the SIP is an operation that perturbs the switching instant t_1 to a neighboring value h while at the same time changes the time t_f accordingly to a certain value \hat{t}_f to maintain the same trajectory boundary values, i.e., $\hat{q}(0) = q_1$ and $\hat{q}(\hat{t}_f) = q_2$. Fig. 4 illustrates an example of obtaining $\mathcal{H}_h[z]$ from $z(t)$. It can be seen that the new trajectory $\mathcal{H}_h[z]$ switches from mode σ_1 to mode σ_2 at time h instead of t_1 and ends at time \hat{t}_f when its continuous state hits q_2 . Mathematically, the perturbed trajectory $\mathcal{H}_h[z] = (\hat{q}(t), \hat{\sigma}(t))$ can be defined as

$$\hat{\sigma}(t) = \begin{cases} \sigma_1 & , t \leq h \\ \sigma_2 & , h < t \leq \hat{t}_f \end{cases}, \quad (4)$$

$$\frac{d\hat{q}(t)}{dt} = r_{\hat{\sigma}(t)} - r_y, \quad \text{for } t \in [0, \hat{t}_f],$$

$$\text{and } \hat{t}_f = h + \frac{h(r_y - r_{\sigma_1}) + q_2 - q_1}{r_{\sigma_2} - r_y}.$$

Under the above notations, a SIP $\mathcal{H}_h[z]$ is called *valid* if

$$0 \leq h \leq \hat{t}_f \quad \text{and} \quad \hat{q}(t) \in [0, Q] \quad \forall t \in [0, \hat{t}_f]. \quad (5)$$

In other words, $\mathcal{H}_h[z]$ is valid if it spends nonnegative time in each mode and it does not cause any buffer overflow or underflow. The set of h for which $\mathcal{H}_h[z]$ is valid is called the *domain of h* and is denoted by D_h . Thus for any $h \in D_h$, $\hat{z} = \mathcal{H}_h[z]$ defined in (4) satisfies the following properties:

- 1) \hat{z} follows the same switching sequence (σ_1, σ_2) as z and spends nonnegative time in each mode.
- 2) $\hat{q}(0) = q(0) = q_1$ and $\hat{q}(\hat{t}_f) = q(t_f) = q_2$.
- 3) $\hat{q}(t) \in [0, Q]$ for all $t \in [0, \hat{t}_f]$.

Note that D_h is a bounded connected interval. For example, consider the trajectory z_1 as shown in Fig. 5-(a). Let $(\hat{q}(t), \hat{\sigma}(t)) = \mathcal{H}_h[z_1](t)$. If $h < a$, then \hat{t}_f as defined in (4) will be less than h , which

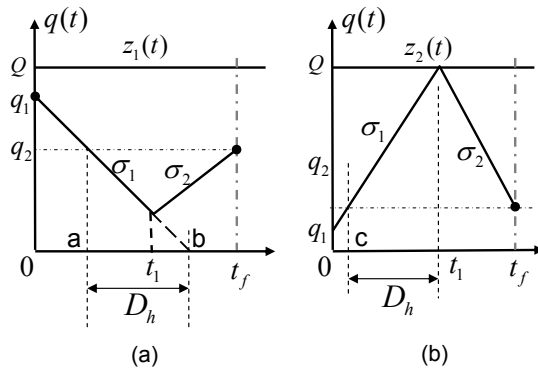


Fig. 5. Range of SIP in two typical cases

violates the first condition in (5). On the other hand, if $h > b$, then $\hat{q}(t) < 0$ for $t \in (b, h]$, which violates the second condition in (5). Hence, $D_h = [a, b]$ for z_1 . As another example, consider the trajectory z_2 as shown in Fig. 5-(b) for which $q(t_1)$ is on the boundary of $[0, Q]$. By a similar argument as in the first example, the range of h for z_2 is $D_h = [c, t_1]$. It is observed from these two examples that if $q(t_i) \in (0, Q)$, then t_1 is an interior point of D_h . On the other hand, if $q(t_i) = 0$ or Q , then t_i is on the boundary of D_h . This property actually holds for the SIP of arbitrary two-switching trajectories.

The SIP is a specific yet useful operation. Since it can perturb the switching instant without affecting the boundary values ($q(0)$ and $q(t_f)$) and the buffer size Q , it can be used, together with other operations such as cropping and joining, to study the effect of perturbing only one switching instant of a general trajectory.

IV. OPTIMAL PERIODIC SOLUTION

In this section, we derive the optimal solutions of Problem 2 (denoted by OS2 for simplicity). The following lemma can greatly simplify the problem and is crucial for later proofs.

Lemma 2: If z is an OS2, then $z \in \Omega$. In other words, optimal solutions to Problem 2 must be boundary-switching trajectories.

Proof: The key idea of the proof is to use the operations defined in Section III to construct a better trajectory with less power consumption for any given trajectory that has switchings at some interior points of $[0, Q]$. Let $(z(t), Q, T)$ be a solution to Problem 2. Denote by $(\sigma_1, \dots, \sigma_{n_T})$ and (t_1, \dots, t_{n_T}) the switching sequence and switching instants in the first period of $z(t)$. Suppose that $z(t)$ has a switching at some interior point of $[0, Q]$, i.e., $0 < q(t_i) < Q$ for some i . Divide the first period of $z(t)$ into three

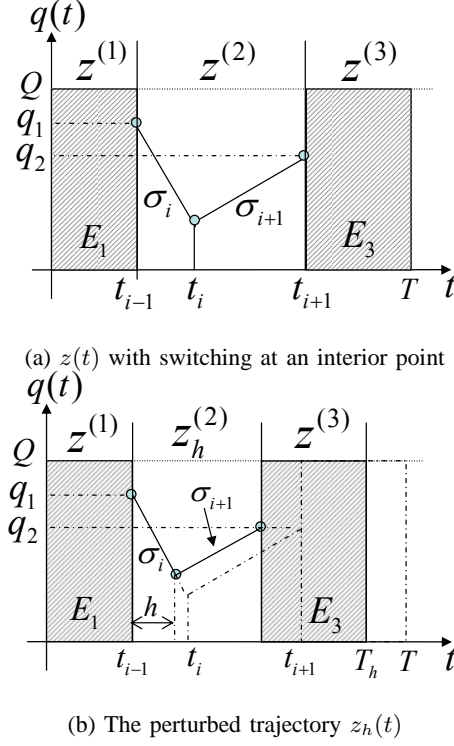


Fig. 6. Scheme of variation

parts through the cropping operation as shown in Fig. 6-(a):

$$z^{(1)}(t) = \mathcal{C}_{0,t_{i-1}}[z](t), \quad z^{(2)}(t) = \mathcal{C}_{t_{i-1},t_{i+1}}[z](t),$$

and $z^{(3)}(t) = \mathcal{C}_{t_{i+1},T}[z](t).$ (6)

Assume that $z^{(2)}(t) = (q^{(2)}(t), \sigma^{(2)}(t))$, $q^{(2)}(0) = q_1$ and $q^{(2)}(t_{i+1} - t_{i-1}) = q_2$. Perform the SIP on $z^{(2)}$ to obtain a new trajectory $z_h^{(2)} = (q_h^{(2)}(t), \sigma_h^{(2)}(t)) \triangleq \mathcal{H}_h[z^{(2)}]$. According to (4), the length of $z_h^{(2)}$ is

$$t_h^{(2)} = h + \frac{h(r_y - r_{\sigma_i}) + q_2 - q_1}{r_{\sigma_{i+1}} - r_y}. \quad (7)$$

By definition, the SIP does not change the boundary values of $z^{(2)}$, i.e., $q_h^{(2)}(0) = q_1$ and $q_h^{(2)}(t_h^{(2)}) = q_2$. Thus we can rejoin $z^{(1)}$, $z_h^{(2)}$ and $z^{(3)}$ as shown in Fig. 6-(b) to obtain

$$z_h \triangleq \mathcal{J}[z^{(1)}, z_h^{(2)}, z^{(3)}]. \quad (8)$$

It is obvious that the length of z_h is

$$T_h = t_{i-1} + t_h^{(2)} + (T - t_{i+1}). \quad (9)$$

Now we show that z_h consumes less power than z for some h . Recall that D_h is the set of h that $z_h^{(2)}$ remains valid. According to (5), Q is a valid buffer size for z_h if $h \in D_h$. Thus $\forall h \in D_h$ the power of

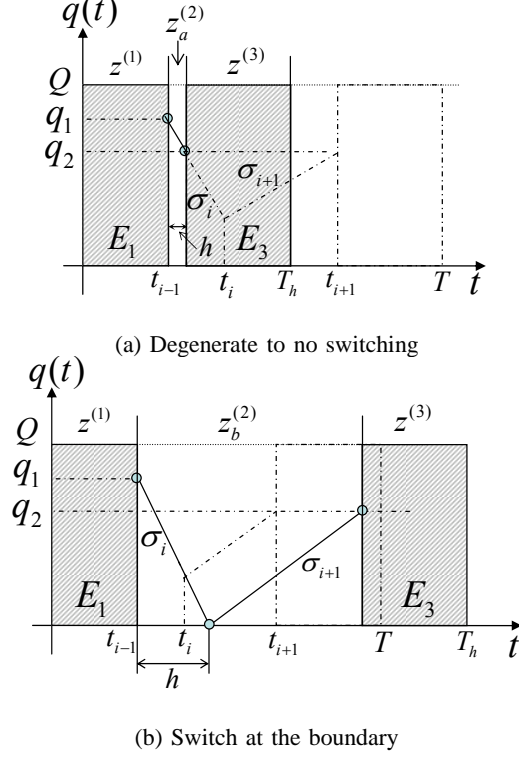


Fig. 7. Two Extreme Cases of Variations on t_i

z_h with buffer size Q is

$$\begin{aligned} \bar{P}(z_h; Q, T_h) = & \frac{1}{T_h} [E_1 + E_3 + n_T k_s + p_{\sigma_i} \cdot h \\ & + p_{\sigma_{i+1}} (t_h^{(2)} - h)] + p_b Q, \end{aligned} \quad (10)$$

where E_1 and E_3 are the running energy of $z^{(1)}$ and $z^{(3)}$, respectively. Taking the derivative of $\bar{P}_h(z_h; Q, T_h)$ with respect to h , we have

$$\begin{aligned} \frac{d\bar{P}(z_h; Q, T_h)}{dh} = & \frac{1}{(T_h)^2} \left[\left(p_{\sigma_i} + p_{\sigma_{i+1}} \frac{r_y - r_{\sigma_i}}{r_{\sigma_{i+1}} - r_y} \right) \right. \\ & \cdot \left(T - (t_{i+1} - t_{i-1}) + \frac{q_2 - q_1}{r_{\sigma_{i+1}} - r_y} \right) - \left(1 + \frac{r_y - r_{\sigma_i}}{r_{\sigma_{i+1}} - r_y} \right) \\ & \left. \cdot \left(E_1 + E_3 + n_T k_s + p_{\sigma_{i+1}} \frac{q_2 - q_1}{r_{\sigma_{i+1}} - r_y} \right) \right]. \end{aligned} \quad (11)$$

Note that the h -related terms in the numerator have been cancelled out. Suppose that $D_h = [a, b]$. Since $q(t_i) \in (0, Q)$ by assumption, $t_i \in (a, b)$ as discussed in Section III-F. From (11) it is clear that the sign of $\frac{d\bar{P}(z_h; Q, T_h)}{dh}$ does not depend on h , which indicates that $\bar{P}(z_h; Q, T_h)$ is monotone with respect to h in $[a, b]$. Thus either z_a (Fig. 7-(a)) or z_b (Fig. 7-(b)) consumes less power than z . Without loss of

generality, assume z_a consumes less power than z . Then the periodic extension of z_a , $\mathcal{P}[z_a]$, is a better periodic solution to Problem 2 than z . Thus it follows that $q(t_i) = 0$ or Q for all $i = 1, \dots, n_T$, i.e., the OS2 must be a BST. ■

Lemma 2 enables one to focus on the BST's (Ω) in deriving the optimal solutions to Problem 2. Recall that the variable n_p is used to describe the purity of a BST. In the rest of this section, we will first solve a simple case of Problem 2 where only the pure periodic trajectories with $n_p = 1$ are considered as candidate solutions. Then we will prove that the solution in this simple case is actually an OS2 for an arbitrary n_p .

A. Optimal Pure Periodic Trajectory (OPPT)

The *Optimal pure periodic trajectory (OPPT)* is defined as the optimal periodic solution to Problem 2 under an additional constraint $n_p = 1$, i.e., the candidate trajectories must be pure boundary-switching trajectories. Let z be a periodic trajectory satisfying this condition. Then every period of z consists of the same Λ -pair. Thus the main task of this subsection is to find the best Λ -pair and the best period T of z .

For a given Λ -pair $\{i, j\}$, the period T_{ij} can be expressed in terms of the corresponding buffer size Q_{ij} as

$$T_{ij} = \frac{Q_{ij}}{r_i - r_y} + \frac{Q_{ij}}{r_y - r_j} \triangleq \alpha_{ij} Q_{ij}. \quad (12)$$

Denote by β_{ij} the running power of z over a period, i.e.,

$$\beta_{ij} = \frac{1}{T_{ij}} \left[\frac{Q_{ij} p_i}{r_i - r_y} + \frac{Q_{ij} p_j}{r_y - r_j} \right] = \frac{1}{\alpha_{ij}} \left[\frac{p_i}{r_i - r_y} + \frac{p_j}{r_y - r_j} \right]. \quad (13)$$

Note that both α_{ij} and β_{ij} are constants depending only on the given Λ -pair. With these notations, the average power of z over one period is given by

$$\bar{P}_{ij}^T(Q_{ij}) = \beta_{ij} + \frac{2k_s}{\alpha_{ij} Q_{ij}} + p_b Q_{ij}. \quad (14)$$

Taking the derivative of (14) with respect to Q_{ij} and setting it to zero, we obtain the optimal buffer size for the Λ -pair $\{i, j\}$ as:

$$Q_{ij}^* = \sqrt{\frac{2k_s}{\alpha_{ij} p_b}}. \quad (15)$$

Thus the minimum achievable power for the Λ -pair $\{i, j\}$ is $\bar{P}_{ij}^T(Q_{ij}^*)$. The optimal Λ -pair $\{\sigma_T^+, \sigma_T^-\}$ can be obtained by minimizing $\bar{P}_{ij}^T(Q_{ij}^*)$ with respect to $\{i, j\}$, i.e.,

$$\{\sigma_T^+, \sigma_T^-\} = \arg \min_{\{i \in I, j \in J\}} \bar{P}_{ij}^T(Q_{ij}^*). \quad (16)$$

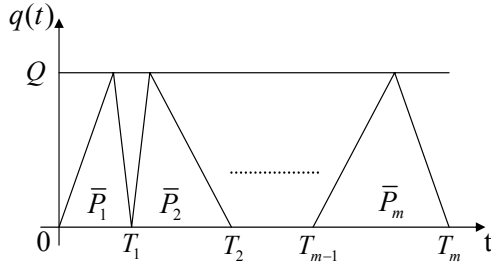


Fig. 8. A boundary-switching trajectory with $n_T > 2$

Since solving (16) entails comparison of at most $N(N - 1)/2$ quantities, the computational cost for obtaining the best Λ -pair is fairly low. Note that the minimizers in (16) may not be unique. Denote by Σ the set of all the minimizers in (16) and by $|\Sigma|$ the number of elements in Σ . Two or more elements in Σ are called *equivalent Λ -pairs* if they correspond to the same optimal buffer size as defined in (15). In other words, the equivalent Λ -pairs are the Λ -pairs that minimize (16) with the same optimal buffer size. The following theorem summarizes the above results and gives a rigorous definition of the OPPTs.

Theorem 1: Let $z(t)$ be a pure periodic trajectory with (i, j) and $(0, \frac{Q}{r_i - r_j})$ as the switching sequence and switching instants in its first period, respectively. If $\{i, j\} \in \Sigma$ and $Q = Q_{ij}^*$ as defined in (15), then z is an OPPT with period T_{ij} .

B. General Optimal Solutions

In this section, we will prove that the OPPT derived in the last section for the case $n_p = 1$ is actually an OS2 for an arbitrary n_p . Furthermore, if Σ contains equivalent Λ -pairs, then the OPPT can be used as a building block to construct more complicated OS2s that are not pure. The main result of this section is the following theorem.

Theorem 2: The OPPT defined in Theorem 1 is an OS2.

Proof: Let $z^*(t)$ be an OPPT as defined in Theorem 1 and \bar{P}^* be its average power. Let $z(t) = (q(t), \sigma(t))$ be an arbitrary periodic trajectory with average power \bar{P} . We need to show that $\bar{P}^* \leq \bar{P}$. According to Lemma 2, we can assume $z \in \Omega$. If z is pure, then by the definition of z^* , we automatically have $\bar{P}^* \leq P$. Hence, we assume that z is mixed with $n_p > 1$ and its first period is as shown in Fig 8. Let $T_i, i = 0, \dots, m$, be the successive time instants such that $q(T_i) = 0$. Denote by $\bar{P}_i, i = 1, \dots, m$, the average power of $\mathcal{C}_{T_{i-1}, T_i}[z]$, which is the part of $z(t)$ within the interval $[T_{i-1}, T_i)$. It is obvious that $\bar{P} = \frac{\bar{P}_1 T_1 + \dots + \bar{P}_m (T_m - T_{m-1})}{T_m}$ is a convex combination of $\bar{P}_1, \dots, \bar{P}_m$. Thus $\bar{P} \geq \bar{P}_{i^*}$, where $i^* = \arg \min_i \bar{P}_i$.

Furthermore, we also have $\bar{P}_{i^*} \geq \bar{P}^*$, as otherwise the periodic extension of $\mathcal{C}_{T_{i^*-1}, T_{i^*}}[z]$ is also pure but consumes less power than z^* , which contradicts the optimality of z^* . Hence, $\bar{P}^* \leq \bar{P}_{i^*} \leq \bar{P}$. ■

When $|\Sigma| > 1$, the OPPT is not unique and neither is the OS2 according to Theorem 2. Furthermore, if Σ contains equivalent Λ -pairs, we can use them to even construct an OS2 that is not pure. To see this, let z_1 and z_2 be two different OPPTs consisting of equivalent Λ -pairs with optimal buffer sizes Q_1 and Q_2 , optimal period T_1 and T_2 and average power \bar{P}_1 and \bar{P}_2 , respectively. By the definition of the equivalent Λ -pairs, we must have $\bar{P}_1 = \bar{P}_2$ and $Q_1 = Q_2$. Define $\hat{z}_1 = \mathcal{C}_{0, T_1}[z_1]$, $\hat{z}_2 = \mathcal{C}_{0, T_2}[z_2]$ and $z = \mathcal{P}[\mathcal{J}[\hat{z}_1, \hat{z}_2]]$. In other words, z is a periodic trajectory with each period defined by connecting one period of z_1 and z_2 together. It is obvious that z consumes the same average power as z_1 and z_2 . Thus z is an OS2 with two different Λ -pairs, i.e., $n_p = 2$. In a similar way, more complicated OS2s can be constructed if Σ contains more than two equivalent Λ -pairs.

Although mixed OS2s may exist, the OPPT is the simplest OS2 which can be easily computed and implemented. Thus we will focus on the OPPT in the rest of this paper for optimal solutions of Problem 2.

C. t_f -adapted OPPT

The OPPT is an infinite-length periodic trajectory that requires an infinite amount of incoming data. However, for real applications, the amount of data to be transferred is finite. Therefore, when the OPPT is used in a real application, another guard condition should be added to the system: switch component X to the lowest power mode (mode 1) whenever there is no more incoming data. Suppose that for an application, X needs to produce $t_f r_y$ amount of data for Y and this amount is not known during the design process. In this case, we can solve Problem 2 to obtain an OPPT $z_T = (q(t), \sigma(t))$ with period T . To evaluate how well z_T performs for this application, define the t_f -adapted trajectory, denoted by $\mathcal{A}_{t_f}[z_T]$, as

$$\begin{aligned} \mathcal{A}_{t_f}[z_T] &= (\hat{q}(t), \hat{\sigma}(t)), \\ \text{where } \hat{\sigma}(t) &= \begin{cases} \sigma(t) & , t \leq t_s \\ 1 & , t_s < t \leq t_f \end{cases}, \\ \text{and } \frac{d\hat{q}(t)}{dt} &= \begin{cases} r_{\hat{\sigma}(t)} - r_y & , t \leq t_s \\ -r_y & , t_s < t \leq t_f \end{cases}, \end{aligned} \quad (17)$$

where $t_s \neq t_f$ is the unique solution of equation $q(t_s) = (t_f - t_s)r_y$. In other words, $\mathcal{A}_{t_f}[z_T]$ follows exactly the original trajectory z_T until the time t_s when X finishes producing the $t_f r_y$ amount of data. During the interval $[t_s, t_f]$, component X is switched to the lowest power mode consuming a constant

power p_1 , while component Y is reading the remaining data in the buffer. Note that regardless of whether r_1 is 0 or not, X is not producing any new data during $[t_s, t_f]$ as all the $t_f r_y$ amount of data has been sent to the buffer before t_s . The $\mathcal{A}_{t_f}[z_T]$ reflects what actually happens to the system when the strategy z_T is applied to a real application with unknown but finite duration t_f . Although it is obtained based on the optimal periodic trajectory z_T , it may not be optimal for this particular application unless t_f is an integer multiple of T .

V. OPTIMAL SOLUTIONS FOR FIXED AND GIVEN t_f

For unknown t_f , the OPPT is a good switching policy since it is the best periodic strategy that can be easily implemented by computers (resulting in a t_f -adapted trajectory). In this section, we study the case where the exact value of t_f is known and derive optimal solutions to Problem 1 (OS1). An OS1 can be used to construct a periodic trajectory with period t_f through the periodic extension. In this sense, Problem 1 can be thought of as a version of Problem 2 with a fixed period $T = t_f$. With the constraint for the period, Problem 1 becomes more difficult than Problem 2. On the other hand, with the additional knowledge of t_f , we expect to obtain a solution that performs even better than the t_f -adapted OPPT for this particular t_f .

Not surprisingly, the optimal solution to Problem 1 must also be a boundary-switching trajectory.

Lemma 3: If z is an OS1, then $z \in \Omega$.

Remark 2: The perturbed trajectory z_h defined in (8) plays an important role in the proof of Lemma 2. However, since z_h has a different length from z , it can not be directly applied to prove Lemma 3 where the time horizon t_f is given and fixed. The key idea of the proof of Lemma 3 is to further perturb z_h using scaling operation with a proper parameter c so that $\mathcal{S}_c[z_h]$ has the same length as z and then show that the average power of $\mathcal{S}_c[z_h]$ is less than that of z for certain h if z has interior switchings. Refer to Appendix for a complete proof.

Lemma 3 enables one to consider only the BST's in finding the OS1's. Similar to the periodic case, in the rest of this section, we will first find a solution in a simple case where $n_p = 1$ and then prove that this solution is also an OS1 for an arbitrary n_p .

A. Optimal Pure Trajectory (OPT)

The *optimal pure trajectory (OPT)* is defined as the optimal solution to Problem 1 under an additional constraint $n_p = 1$, i.e., only pure trajectories are considered as candidate solutions. As discussed in Section III-E, any finite-length pure trajectory can be thought of as obtained from a Λ -trajectory through

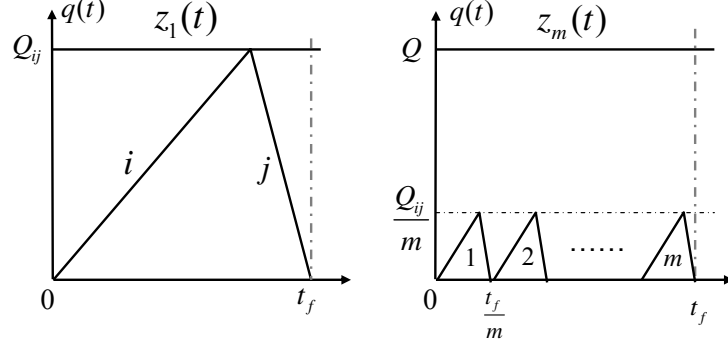


Fig. 9. Obtaining z_m from z_1 through folding

a folding operation. Thus the main task is to determine the best Λ -pair and the corresponding best folding parameter.

Let $z_1(t)$ be a Λ -trajectory with length t_f and Λ -pair $\{i, j\}$. Since t_f is fixed, its optimal buffer size is given by:

$$Q_{ij} = \frac{t_f}{\alpha_{ij}}, \quad (18)$$

where α_{ij} is the constant defined in (12). Define $z_m = \mathcal{F}_m[z_1]$. Then z_m is a pure trajectory as shown in Fig. 9 with $2m$ switchings and the same Λ -pair as z_1 . As discussed in Section III-E, z_m has an optimal buffer size Q_{ij}/m and its average power is

$$\bar{P}_{ij}^{t_f}(m) = \beta_{ij} + \frac{2mk_s}{t_f} + \frac{p_b t_f}{m\alpha_{ij}}, \quad (19)$$

where β_{ij} is the constant defined in (13). Taking the derivative of $\bar{P}_{ij}^{t_f}$ with respect to m and setting it to zero, we obtain the optimal value of m as

$$\hat{m}_{ij} = t_f \sqrt{\frac{p_b}{2k_s \alpha_{ij}}}. \quad (20)$$

Note that the folding parameter m must be an integer, and the function $\bar{P}_{ij}^{t_f}(m)$ is convex in m . Therefore, if \hat{m}_{ij} is not an integer, the optimal feasible value of m_{ij} , m_{ij}^* , is whichever of the two neighboring integers of \hat{m}_{ij} that results in a smaller value of $\bar{P}_{ij}^{t_f}(m)$ as defined in (19). Hence,

$$m_{ij}^* = \arg \min_{m \in \{\lfloor \hat{m}_{ij} \rfloor, \lceil \hat{m}_{ij} \rceil\}} \bar{P}_{ij}^{t_f}(m). \quad (21)$$

The minimal achievable power with the Λ -pair $\{i, j\}$ is $\bar{P}_{ij}^{t_f}(m_{ij}^*)$. Then the best Λ -pair $\{\sigma_{t_f}^+, \sigma_{t_f}^-\}$ can be obtained as

$$\{\sigma_{t_f}^+, \sigma_{t_f}^-\} = \arg \min_{\{i \in I, j \in J\}} \bar{P}_{ij}^{t_f}(m_{ij}^*). \quad (22)$$

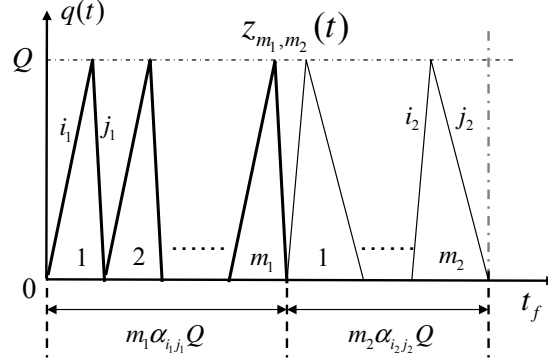


Fig. 10. An example of $z_{m_1, m_2}(t)$

Denote by Σ_f the set of all minimizers of (22) and by $|\Sigma_f|$ the number of elements in Σ_f . The following theorem summarizes the above results.

Theorem 3: Let $z_m(t)$ be a pure trajectory as shown in the right side of Fig. 9 with $2m$ switchings and Λ -pair $\{i, j\}$. If $\{i, j\} \in \Sigma_f$ and $m = m_{i, j}^*$, then z_m is an OPT with optimal buffer size Q_{ij}/m_{ij}^* .

B. General Optimal Solution

In last subsection, we derive analytically the optimal pure trajectories with $n_p = 1$. A natural question is that whether the power can be further reduced if we relax the constraint on n_p . To answer this question, we start with a simple case where the candidate trajectories are allowed to contain at most two distinct Λ -pairs,⁴ i.e., $n_p \leq 2$. Let z_{m_1, m_2} be a BST consisting of m_1 copies of Λ -pair (i_1, j_1) and m_2 copies of Λ -pair (i_2, j_2) . Without loss of generality, assume that all the same pairs are grouped together as shown in Fig 10. In other words, the switching sequence of z_{m_1, m_2} is assumed to be

$$(\sigma_1, \dots, \sigma_{2(m_1+m_2)}) = (\underbrace{i_1, j_1, \dots, i_1, j_1}_{m_1 \text{ pairs}}, \underbrace{i_2, j_2, \dots, i_2, j_2}_{m_2 \text{ pairs}}).$$

The optimal buffer size of z_{m_1, m_2} is uniquely determined by $Q = \frac{t_f}{\alpha_{i_1, j_1} m_1 + \alpha_{i_2, j_2} m_2}$, where $\alpha_{i, j}$ is the constant defined in (12). Let $\beta_{i, j}$ be the running power of the Λ -pair $\{i, j\}$ as defined in (13). Then the

⁴Two different Λ -pairs may consist of three or four different modes. For example, $\{\sigma_1, \sigma_2\}$ and $\{\sigma_1, \sigma_3\}$ are also called two different Λ -pairs although they have one mode in common.

total energy consumed by z_{m_1, m_2} is computed as

$$E(m_1, m_2) = 2(m_1 + m_2)k_s + \frac{p_b t_f^2 + \beta_{i_1, j_1} \alpha_{i_1, j_1} m_1 t_f + \beta_{i_2, j_2} \alpha_{i_2, j_2} m_2 t_f}{\alpha_{i_1, j_1} m_1 + \alpha_{i_2, j_2} m_2}.$$

Lemma 4: For any $\{i_1, j_1\}$ and $\{i_2, j_2\}$, there exists a pair of nonnegative integers (m_1^*, m_2^*) with either $m_1^* = 0$ or $m_2^* = 0$ such that $E(m_1^*, m_2^*) \leq E(m_1, m_2)$, for any other pair of nonnegative integers (m_1, m_2) ,

Proof: For simplicity, define $a_1 = \beta_{i_1, j_1} \alpha_{i_1, j_1} t_f$, $a_2 = \beta_{i_2, j_2} \alpha_{i_2, j_2} t_f$ and $c = p_b t_f^2$. Relax m_1, m_2 to nonnegative real numbers x_1 and x_2 . Then

$$E(x_1, x_2) = 2k_s(x_1 + x_2) + \frac{a_1 x_1 + a_2 x_2 + c}{\alpha_{i_1, j_1} x_1 + \alpha_{i_2, j_2} x_2}.$$

Note that all the constants $a_1, a_2, c, \alpha_{i_1, j_1}$, and α_{i_2, j_2} are positive. To prove the lemma, it suffices to show that there exists a point on the x_1 or x_2 axis that minimizes $E(x_1, x_2)$ in the first quadrant. To find the minimizers of $E(x_1, x_2)$ in the first quadrant, we can first minimize it along each ray in the first quadrant, and then find the ray that gives the best minimum value. Towards this purpose, consider $x_2 = \lambda x_1$, where $\lambda \in [0, \infty]$. Then

$$\begin{aligned} E(x_1, \lambda x_1) &= 2k_s(1 + \lambda)x_1 + \frac{(a_1 + a_2\lambda)x_1 + c}{(\alpha_{i_1, j_1} + \alpha_{i_2, j_2}\lambda)x_1} \\ &\geq 2\sqrt{\frac{2k_s(1 + \lambda)c}{\alpha_{i_1, j_1} + \alpha_{i_2, j_2}\lambda}} + \frac{(a_1 + a_2\lambda)}{(\alpha_{i_1, j_1} + \alpha_{i_2, j_2}\lambda)} \\ &\triangleq E(x_1^*, \lambda x_1^*). \end{aligned}$$

Thus $E(x_1^*, \lambda x_1^*)$ is the minimum value achieved on the ray $x_2 = \lambda x_1$. To prove the lemma, it suffices to show that either $\lambda = 0$ or $\lambda = \infty$ minimizes $E(x_1^*, \lambda x_1^*)$. After some computations, $E(x_1^*, \lambda x_1^*)$ reduces to

$$E(x_1^*, \lambda x_1^*) = d_3 \sqrt{d_2 y + \frac{1}{\alpha_{i_2, j_2}}} + d_1 y + \frac{a_2}{\alpha_{i_2, j_2}} \triangleq f(y),$$

where $y = \frac{1}{\alpha_{i_2, j_2}^2 \lambda + \alpha_{i_1, j_1} \alpha_{i_2, j_2}}$ and $d_1 = a_1 \alpha_{i_2, j_2} - a_2 \alpha_{i_1, j_1}$, $d_2 = \alpha_{i_2, j_2} - \alpha_{i_1, j_1}$ and $d_3 = 2\sqrt{2k_s c}$ are all constants. Note that except d_1 and d_2 , all the other constants are positive. As λ increases from 0 to ∞ , y decreases from $\frac{1}{\alpha_{i_1, j_1} \alpha_{i_2, j_2}}$ to 0. Hence, it suffices to show that either 0 or $\frac{1}{\alpha_{i_1, j_1} \alpha_{i_2, j_2}}$ is a minimizer of $f(y)$ in $[0, \frac{1}{\alpha_{i_1, j_1} \alpha_{i_2, j_2}}]$. Note that the second-order derivative of $f(y)$ is

$$\frac{d^2 f}{dy^2}(y) = -\frac{d_2^2 d_3}{4(d_2 y + 1/\alpha_{i_2, j_2})^{3/2}} \leq 0.$$

Thus $f(y)$ is a concave function of y in $[0, \frac{1}{\alpha_{i_1, j_1} \alpha_{i_2, j_2}}]$. Since the minimizer of a concave function over a bounded set must be on the boundary of the set, we conclude that either 0 or $\frac{1}{\alpha_{i_1, j_1} \alpha_{i_2, j_2}}$ is a minimizer of $f(y)$ in $[0, \frac{1}{\alpha_{i_1, j_1} \alpha_{i_2, j_2}}]$. ■

According to Lemma 4, for any given two Λ -pairs, we can always use one of them to construct a pure trajectory that performs equally well or better than all the other mixed trajectories involving these two Λ -pairs. Therefore, the following corollary follows immediately.

Corollary 1: The OPT is an optimal solution to Problem 1 under an additional constraint $n_p \leq 2$.

The question now becomes that whether more energy can be saved by further relaxing the constraint on n_p . It turns out to be not the case. In fact, the OPT is an optimal solution to Problem 1 for an arbitrary n_p . This can be proved by induction. The following lemma is the key of the induction procedure.

Lemma 5: For any BST z with length t_f and $n_p = l + 1$, there exists another BST \hat{z} with length t_f and $n_p \leq l$ that consumes equal or less power than z .

The proof of Lemma 5 can be found in Appendix . By this lemma, any BST corresponds to a pure trajectory with no more power consumption. Thus the following theorem follows immediately.

Theorem 4: The OPT defined in Theorem 3 is an OS2 for an arbitrary n_p .

C. OPT vs. (t_f -adapted) OPPT

In this subsection, we compare the OPT derived in last subsection with the (t_f -adapted) OPPT derived in Section IV to get a clearer picture of how the corresponding two problems, initially formulated from two different practical aspects, relate to each other.

Proposition 1: Let z_T be an OPPT with period T and z_{t_f} be an OPT with length t_f and $2m$ switchings. Denote by $z_T^{t_f}$ the t_f -adapted trajectory of z_T . Let $\bar{P}(\cdot)$ be the average power for a given trajectory. Then the three trajectories satisfy:

- 1) $\bar{P}(z_T) \leq \bar{P}(z_{t_f}) \leq \bar{P}(z_T^{t_f})$ for any $t_f \geq 0$;
- 2) If $t_f = l \cdot T$ for some $l \in \mathbb{N}$, then $\bar{P}(z_{t_f}) = \bar{P}(z_T) = \bar{P}(z_T^{t_f})$;
- 3) $\bar{P}(z_{t_f}) \rightarrow \bar{P}(z_T)$ and $\bar{P}(z_T^{t_f}) \rightarrow \bar{P}(z_T)$ as $t_f \rightarrow \infty$.

Proof: (i) Obviously $\bar{P}(z_{t_f}) \leq \bar{P}(z_T^{t_f})$ as $z_T^{t_f}$ is also a trajectory with length t_f . Since z_T is the best periodic trajectory, $\bar{P}(z_T) \leq \bar{P}(\mathcal{P}[z_{t_f}]) = \bar{P}(z_{t_f})$. The desired result follows. (ii) Obviously $\bar{P}(z_T) = \bar{P}(z_T^{t_f})$ as $z_T^{t_f}$ is just the first l periods of z_T . Considering the result in (i), all the three powers are equal. (iii) According to (i), it suffices to prove that $\bar{P}(z_T^{t_f}) \rightarrow \bar{P}(z_T)$ as $t_f \rightarrow \infty$. Let $m_{t_f} = \lfloor t_f/T \rfloor$. Then $m_{t_f}T/t_f \rightarrow 1$ as $t_f \rightarrow \infty$. Denote by \bar{P}_1 and \bar{P}_2 the average power of $z_T^{t_f}$ during the interval $[0, m_{t_f}T]$ and $[m_{t_f}T, t_f]$, respectively. According to (17), $t_s > m_{t_f}T$ and $z_T^{t_f}(t) = z_T(t)$ for

TABLE I
POWER MODES OF SYSTEM H1

mode i	1	2	3	4	5	6
r_i	0	1	2	3	4	5
p_i	0.1	0.12	0.2	0.3	0.33	0.4

$t \in [0, m_{t_f}T]$. Thus $\bar{P}_1 = \bar{P}(z_T)$. Note that $\bar{P}_2 \leq p_N + \frac{2k_s}{t_f - m_{t_f}T} + p_b Q$, where p_N is the power of the highest mode. Hence, as $t_f \rightarrow \infty$,

$$\bar{P}(z_{t_f}^{t_f}) = \frac{\bar{P}_1 m_{t_f}T + \bar{P}_2 (t_f - m_{t_f}T)}{t_f} \rightarrow \bar{P}(z_T).$$

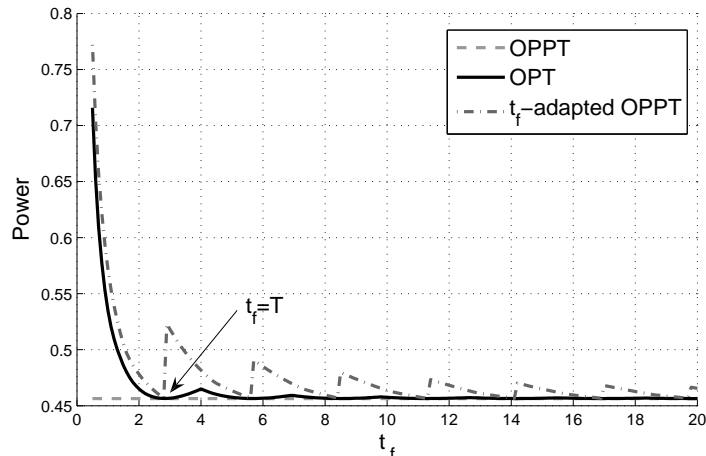
■

Remark 3: Any practical application corresponds to a finite t_f . If the t_f is unknown, we can only compute the OPPT (z_T). Applying z_T to the application results in a t_f -adapted trajectory $z_T^{t_f}$. On the other hand, if t_f is known *a priori*, a better trajectory (z_{t_f}) than $z_T^{t_f}$ can be computed. In fact, z_{t_f} is the best trajectory for the given t_f and its power is bounded from below by $\bar{P}(z_T)$ and from above by $\bar{P}(z_{t_f}^{t_f})$.

VI. SIMULATION

A. Fictional Example

Consider a system (H1) with 6 power modes as defined in Table I. Assume that $k_s = 0.1$, $p_b = 0.1$ and $r_y = 3.5$. For this system H1, we compute the OPPT (z_T), the OPT (z_{t_f}) and the t_f -adapted OPPT ($z_T^{t_f}$), according to Theorem 1, Theorem 4 and equation (17), respectively. Denote by $\bar{P}(\cdot)$ the average power of a given trajectory. In Fig. 11-(a), we plot the power of each trajectory as a function of t_f . It can be seen that $\bar{P}(z_{t_f})$ always stays below $\bar{P}(z_T^{t_f})$ and both of them converge to $\bar{P}(z_T)$ from above as $t_f \rightarrow \infty$. It is also observed that the three trajectories have the same average power when t_f is an integer multiple of the optimal period ($T = 2.8284$) of the OPPT. These observations are consistent with our analysis in Section V-C. In Fig. 11-(b), we plot the optimal Λ -pairs of z_T and z_{t_f} as functions of t_f . It can be seen that the optimal Λ -pair in z_{t_f} is initially $\{5, 2\}$ and eventually converges to $\{5, 4\}$ which is the optimal Λ -pair of z_T (and $z_T^{t_f}$). This indicates that z_{t_f} may involve different Λ -pairs for different t_f .



(a) Convergence of powers

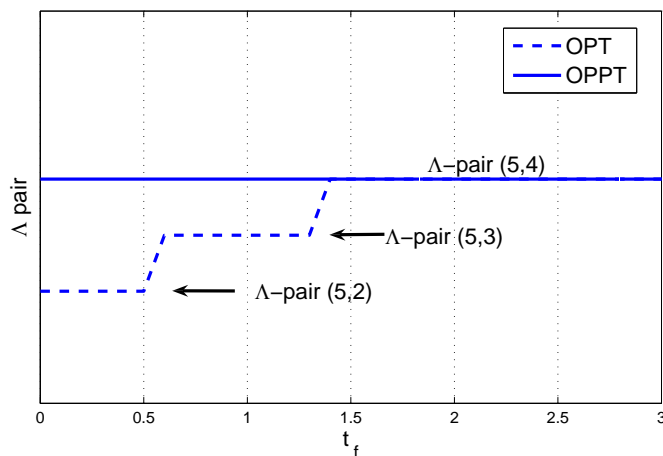
(b) Λ -pairs in the OPPT and OPT

Fig. 11. Simulation results of example 1

B. Practical Example

Our theoretical results can be applied in many real-world applications, such as the power management problem of a multiple-speed disk ([5]) and the dynamic voltage scheduling (DVS) problem of a variable speed processor ([4]). In this section, we use a DVS example to illustrate the effectiveness of our results.

Let X be an Intel Xscal processor ([23]) with five available power modes as defined in Table II. Suppose that Y is a video card that fetches data from X at a constant speed 8 Mbps (1MB/s). The power per megabyte for buffer B can be looked up in the datasheet ([24]) as 6.258×10^{-4} W/MB. A typical value of the switching energy is 0.1mJ in a microprocessor ([4]). Since the switching cost k_s in our model may

TABLE II
POWER MODES OF INTEL XSCALE PROCESSOR

mode i	1	2	3	4	5
f_i (MHz)	150	400	600	800	1000
r_i (MB/s)	0.45	1.2	1.8	2.4	3
p_i (Watt)	0.08	0.17	0.4	0.9	1.6

also include other switching penalties, such as the switching delay penalty, we test our method for k_s ranging from 0.1mJ to 100mJ. As t_f is usually large for video programs, the t_f -adapted OPPT and the OPT will provide almost the same power performance. For simplicity we only implement the t_f -adapted OPPT in this simulation and refer to this method as Scheme 1. A heuristic strategy, referred to as Scheme 2, is also implemented where X is switched to the highest speed until the buffer is full and then switched to the lowest speed until the buffer is empty. Scheme 2 is tested for four heuristically selected buffer sizes 0.1MB, 0.3MB, 1MB and 8MB. The power consumptions of Scheme 2 in these cases are compared with Scheme 1 in Fig. 12. It can be seen that the proposed optimal strategy always performs the best for each k_s and can save about 60% of power consumption compared with the heuristic ones.

VII. CONCLUSIONS

This paper introduces a modeling framework for the DBM problem using hybrid systems. Two practically important DBM problems are formulated as optimal control problems of a piecewise constant hybrid system. Various necessary conditions are derived using some variational approach. It is shown that the optimal pure trajectory (OPT) and the optimal pure periodic trajectory (OPPT) are optimal solutions to Problems 1 and 2, respectively. General guidelines for solving practical DMB problems using these optimal strategies are also discussed. For a particular application, if its time horizon t_f is unknown, one can only compute the OPPT. Applying the OPPT to the application results in a t_f -adapted OPPT, which is a good suboptimal strategy that converges to the true optimal strategy as t_f goes to infinity. On the other hand, if t_f is known, the best strategy OPT can be computed, which guarantees the least energy consumption for this particular application. Future research will focus on the following two aspects: one is to extend our analysis to the case where more than one buffers are inserted among multiple streamlined components. The other one is to study the case where the data rates of components are varying or even random instead of constant.

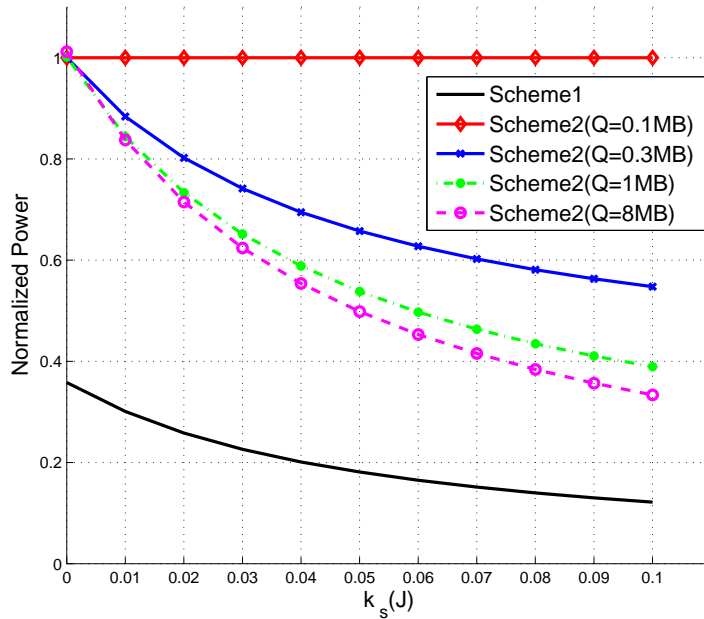


Fig. 12. Power consumptions of various methods under different k_s . For each k_s , all the powers are normalized w.r.t. the largest one.

APPENDIX

Proof: Let $z(t) = (q(t), \sigma(t))$ be an OS1 with switching instants (t_0, \dots, t_{n-1}) and buffer size Q . Suppose $q(t_i) \in (0, Q)$ for some i . Define z_h as in (6) with T replaced by t_f . Then z_h has the same buffer size Q as z , and similar to (9), its length is $t_f^h = t_{i-1} + t_h^{(2)} + (t_f - t_{i+1})$, where $t_h^{(2)}$ is given in (7). Define $\hat{z}_h = \mathcal{S}_{c_h}[z_h]$, where $c_h = t_f/t_f^h$. According to the properties of the scaling operation, the buffer size of \hat{z}_h becomes $c_h Q$ and the length of \hat{z}_h is changed back to t_f . Therefore, \hat{z}_h is a feasible trajectory for Problem 1. Considering (3) and (10), the power of \hat{z}_h is computed as

$$\begin{aligned} \bar{P}(\hat{z}_h; Q, t_f) &= \frac{1}{t_f^h} [E_1 + E_3 + 2k_s + p_{\sigma_i} \cdot h \\ &\quad + p_{\sigma_{i+1}}(t_h^{(2)} - h)] + p_b c_h Q + \frac{nk_s(1 - c_h)}{c_h t_f^h}. \end{aligned}$$

Taking the derivative of $\bar{P}(\hat{z}_h; Q, t_f)$ with respect to h , we have

$$\begin{aligned} \frac{d\bar{P}(\hat{z}_h; Q, t_f)}{dh} &= \frac{1}{(t_f^h)^2} \left[\left(p_{\sigma_i} + p_{\sigma_{i+1}} \frac{r_y - r_{\sigma_i}}{r_{\sigma_{i+1}} - r_y} \right) \right. \\ &\cdot \left(t_f - (t_{i+1} - t_{i-1}) + \frac{q_2 - q_1}{r_{\sigma_{i+1}} - r_y} \right) - \left(1 + \frac{r_y - r_{\sigma_i}}{r_{\sigma_{i+1}} - r_y} \right) \\ &\cdot \left(E_1 + E_3 + k_s + p_{\sigma_{i+1}} \frac{q_2 - q_1}{r_{\sigma_{i+1}} - r_y} \right) \left. \right] \\ &+ \frac{nk_s - p_b Q t_f}{(t_f^h)^2} \left(1 - \frac{r_y - r_{\sigma_i}}{r_{\sigma_{i+1}} - r_y} \right). \end{aligned}$$

Therefore, $\bar{P}(\hat{z}_h; Q, t_f)$ is monotone with respect to h as the sign of $\frac{d\bar{P}(\hat{z}_h; Q, t_f)}{dh}$ does not depend on h . Using the same argument as in the last paragraph of the proof of Lemma 2, it follows that the optimal solution to Problem 1 must also be a BST. \blacksquare

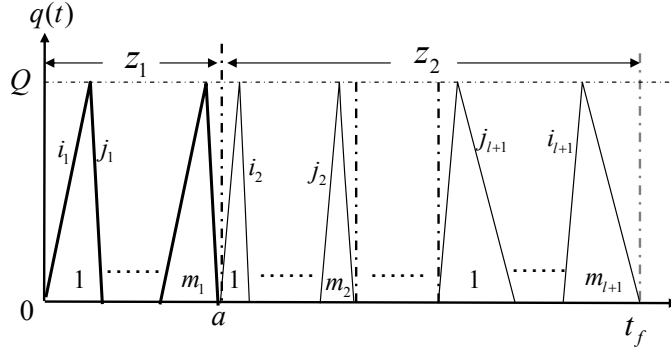


Fig. 13. A trajectory z with $n_p = l + 1$

Proof: Without loss of generality, assume that z is as shown in Fig. 13 with the following switching sequence

$$\underbrace{(i_1, j_1, \dots, i_1, j_1, \dots, i_{l+1}, j_{l+1}, \dots, i_{l+1}, j_{l+1})}_{m_1 \text{ pairs}}.$$

Define $z_1 = \mathcal{C}_{0,a}[z]$ and $z_2 = \mathcal{C}_{a,t_f}[z]$, where a is the starting time of the first copy of $\{i_2, j_2\}$ as shown in Fig. 13. Let $\{\sigma_+, \sigma_-\}$ be a (virtual) Λ -pair whose data rates and powers are defined as

$$\begin{aligned} r_{\sigma_+} &= r_y + \frac{2Q}{t_f}, & r_{\sigma_-} &= r_y - \frac{2Q}{t_f}, \\ p_{\sigma_+} &= \frac{\sum_{k=2}^{l+1} p_{i_k}(\tau_{i_k})}{t_f - a}, & p_{\sigma_-} &= \frac{\sum_{k=2}^{l+1} p_{j_k}(\tau_{j_k})}{t_f - a}, \end{aligned} \tag{23}$$

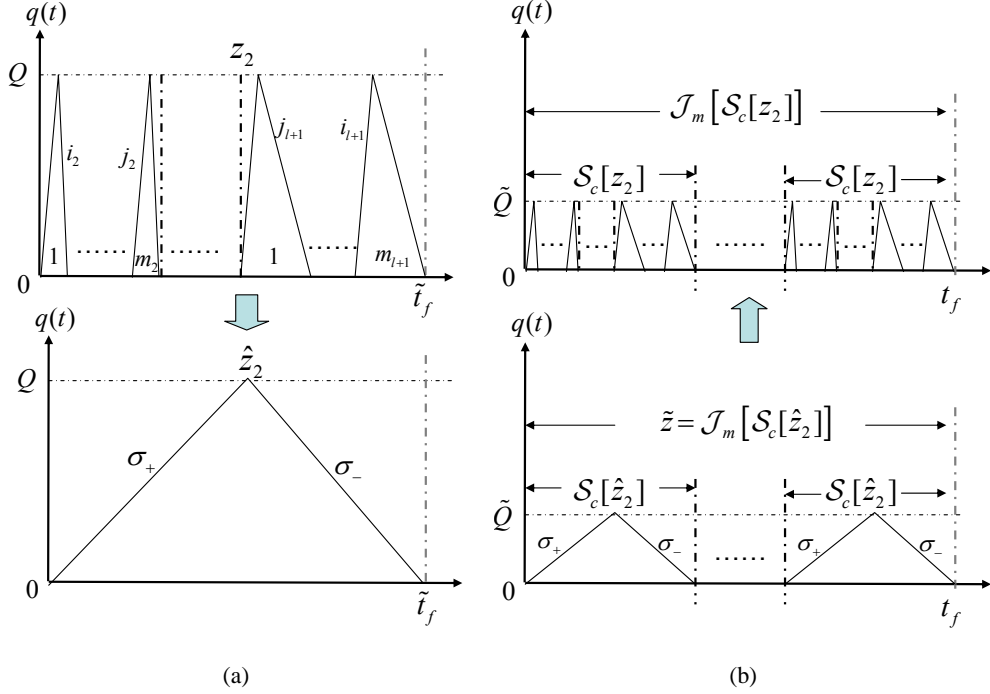


Fig. 14. (a) Two-mode representation of z_2 ; (b) The Optimal trajectory \tilde{z} and its corresponding original trajectory

where τ_{i_k} is the total time z_2 spends in mode i_k . Thus p_{σ_+} and p_{σ_-} in the above equation represent the average powers of all the ascending modes and the descending modes of z_2 , respectively. Note that the so defined modes σ_+ and σ_- may not be feasible modes in S . They are only introduced to simplify the proof. Let \hat{z}_2 be a Λ -trajectory with the virtual modes $\{\sigma_+, \sigma_-\}$ as shown in Fig. 14-(a). Define the switching cost in \hat{z}_2 to be $2lk_s/2$. Then \hat{z}_2 has the same buffer size and total energy as z_2 ; thus $\mathcal{J}[z_1, \hat{z}_2]$ consumes the same energy as z . On the other hand, $\mathcal{J}[z_1, \hat{z}_2]$ is a mixed trajectory with $n_p = 2$; its two different Λ -pairs $\{\sigma_+, \sigma_-\}$ and $\{i_1, j_1\}$ appear 1 and m_1 times, respectively. By Lemma 4, there exists a pure trajectory \tilde{z} involving only the pair $\{i_1, j_1\}$ or $\{\sigma_+, \sigma_-\}$ that consumes no more energy than $\mathcal{J}[z_1, \hat{z}_2]$.⁵ Thus \tilde{z} also consumes no more energy than z . If \tilde{z} involves only the pair $\{i_1, j_1\}$, then it is a pure trajectory ($n_p = 1$) satisfying all the constraints in Problem 1 with no more energy than z . On the other hand, if \tilde{z} involves only the pair $\{\sigma_+, \sigma_-\}$, it may not satisfy the third constraint in Problem 1 as σ_+ and σ_- may not be in S . In this case, \tilde{z} must consist of a series of a scaled version of \hat{z}_2 , i.e., $\tilde{z} = \mathcal{J}_m[\mathcal{S}_c[\hat{z}_2]]$ for some m and c . According to (23), $\mathcal{J}_m[\mathcal{S}_c[z_2]]$ (obtained by replacing every \hat{z}_2

⁵Note that $\{\sigma_+, \sigma_-\}$ and $\{i_1, j_1\}$ have different switching costs. However, with slight modifications, Lemma 4 also applies for the case where the two Λ -pairs have different switching costs.

with z_2) as shown in Fig 14-(b) consumes the same energy as \tilde{z} . Thus we obtain a trajectory $\mathcal{J}_m[\mathcal{S}_c[z_2]]$ with $n_p=l$ (involving only the valid modes $i_2, j_2, \dots, i_{l+1}, j_{l+1}$) that consumes no more energy than z . Hence, in either case we can find a trajectory with $n_p \leq l$ that satisfies all the constraints in Problem 1 and consumes no more power than z . ■

REFERENCES

- [1] L. Cai and Y.-H. Lu, "Energy management using buffer memory for streaming data," *IEEE Transactions on Computer-Aided Design of Integrated Circuits and Systems*, vol. 24, no. 2, pp. 141–152, 2005.
- [2] J. Hu and Y.-H. Lu, "Buffer management for power reduction using hybrid control," in *Proceedings of the IEEE Conference on Decision and Control*, (Seville, Spain), pp. 6997–7002, 2005.
- [3] J. Ridenour, J. Hu, N. Pettis, and Y.-H. Lu, "Low-power buffer management for streaming data," *IEEE Transactions on Circuits and Systems for Video Technology*, vol. 17, no. 2, pp. 143–157, 2007.
- [4] T. D. Burd and R. W. Brodersen, "Design issues for dynamic voltage scaling," in *Proceedings of the international symposium on Low power electronics and design*, pp. 9–14, ACM Press, 2000.
- [5] S. Gurusurthi, A. Sivasubramaniam, M. Kandemir, and H. Franke, "Drpm: Dynamic speed control for power management in server class disks.," in *Proceedings of the International Symposium on Computer Architecture (ISCA)*, pp. 169–179, June 2003.
- [6] R. Alur, T. Henzinger, G. Lafferriere, and G. J. Pappas, "Discrete abstractions of hybrid systems," *Proceedings of the IEEE*, vol. 88, no. 2, pp. 971–984, 2000.
- [7] M. S. Branicky, V. S. Borkar, and S. K. Mitter, "A unified framework for hybrid control: model and optimal-control theory," *IEEE Transactions on Automatic Control*, vol. 43, no. 1, pp. 31–45, 1998.
- [8] S. Hedlund and A. Rantzer, "Optimal control of hybrid system," in *Proceedings of the IEEE Conference on Decision and Control*, vol. 4, (Phoenix, AZ), pp. 3972–3977, December 1999.
- [9] X. Xu and P. Antsaklis, "A dynamic programming approach for optimal control of switched systems," in *Proceedings of the IEEE Conference on Decision and Control*, (Sydney, Australia), pp. 1822–1827, December 2000.
- [10] X. Xu and P. Antsaklis, "Optimal control of switched systems: new results and open problems," in *Proceedings of the American Control Conference*, (Chicago, IL), pp. 2683–2687, June 2000.
- [11] P. Riedinger, F. Kratz, C. Iung, and C. Zanne, "Linear quadratic optimization for hybrid systems," in *Proceedings of the IEEE Conference on Decision and Control*, (Phoenix, AZ), pp. 3059–3064, December 1999.
- [12] P. Riedinger, C. Zanne, and F. Kratz, "Time optimal control of hybrid systems," in *Proceedings of the American Control Conference*, (San Diego, CA), pp. 2466–2470, June 1999.
- [13] H. J. Sussmann, "A maximum principle for hybrid optimal control problems," in *Proceedings of the IEEE Conference on Decision and Control*, (Phoenix, AZ), pp. 425–430, December 1999.
- [14] B. Piccoli, "Hybrid systems and optimal control," in *Proceedings of the IEEE Conference on Decision and Control*, (Tampa, FL), pp. 13–18, December 1998.
- [15] X. Xu and P. Antsaklis, "Optimal control of switched systems based on parameterization of the switching instants," *IEEE Transactions on Automatic Control*, vol. 49, no. 1, pp. 2–16, 2004.
- [16] M. Egerstedt, Y. Wardi, and F. Delmotte, "Optimal control of switching times in switched dynamical systems," *IEEE Transactions on Automatic Control*, vol. 51, no. 1, pp. 110–115, 2006.

- [17] S. C. Bengea and R. A. DeCarlo, "Optimal control of switching systems," *Automatica*, vol. 41, no. 1, pp. 11–27, 2005.
- [18] C. G. Cassandras, D. L. Pepyne, and Y. Wardi, "Optimal control of a class of hybrid systems," *IEEE Transactions on Automatic Control*, vol. 46, no. 3, pp. 398–415, 2001.
- [19] L. Y. Wanga, A. Beydoun, J. Cook, J. Sun, and I. Kolmanovsky, "Optimal hybrid control with applications to automotive powertrain systems," in *Control Using Logic-Based Switching*, vol. 222, (London, UK), pp. 190–200, Springer-Verlag, 1997.
- [20] K. Gokbayrak and C. Cassandras, "A hierarchical decomposition method for optimal control of hybrid systems," in *Proceedings of the IEEE Conference on Decision and Control*, vol. 2, (Sydney, NSW, Australia), pp. 1816–1821, December 2000.
- [21] K. Gokbayrak and C. G. Cassandras, "Hybrid controllers for hierarchically decomposed systems," in *HSCC '00: Proceedings of the Third International Workshop on Hybrid Systems: Computation and Control*, (London, UK), pp. 117–129, Springer-Verlag, 2000.
- [22] Y.-H. Lu, L. Benini, and G. D. Micheli, "Dynamic frequency scaling with buffer insertion for mixed workloads," *IEEE Transactions on Computer-Aided Design of Integrated Circuits and Systems*, vol. 21, no. 11, pp. 1284–1305, 2002.
- [23] R. Xu, C. Xi, R. Melhem, and D. Moss, "Practical pace for embedded systems," in *EMSOFT '04: Proceedings of the 4th ACM international conference on Embedded software*, pp. 54–63, ACM Press, 2004.
- [24] Rambus-Inc., "Rambus 128/144-mbit direct rdram data sheet," June 2000.